D10

N79-15598

CLOSED LOOP MODELS FOR ANALYZING THE EFFECTS OF SIMULATOR CHARACTERISTICS*

by

Sheldon Baron, Ramal Muralidharan, David Kleinman
Bolt Beranek and Newman Inc., Cambridge, MA

ABSTRACT

The optimal control model (OCM) of the human operator is used to develop closed-loop models for analyzing the effects of (digital) simulator characteristics on predicted performance and/or workload. Two approaches are considered: the first utilizes a continuous approximation to the discrete simulation in conjunction with the standard optimal control model; the second involves a more exact discrete description of the simulator in a closed-loop multi-rate simulation in which the optimal control model "simulates" the pilot. Both models predict that simulator characteristics can have significant effects on performance and workload.

1. INTRODUCTION

The development of engineering requirements for man-in-the-loop digital simulation is a complex task involving numerous trade-offs between simulation fidelity and costs, accuracy and speed, etc. The principal issues confronting the developer of a simulation involve the design of the cue (motion and visual) environment so as to meet simulation objectives and the design of the digital simulation model to fulfill the real-time requirements with adequate accuracy.

The design of the simulation model has become increasingly important and difficult as digital computers play a more central role in the simulations. For real-time digital simulation with a pilot in the loop the design problem involves specification of conversion equipment (A-D and D-A) as well as of the discrete model of the system dynamics. The design of an adequate discrete simulation is also related closely to the cue generation problem inasmuch as the errors and, in particular, the delays introduced by the simulation will be present in the information cues utilized by the pilot. The significance of this problem has been amply demonstrated.[1,2] Of course, human pilots can compensate for model shortcomings as well as for those of cue generation, with possible effects on the subjective evaluation of the simulation.

The objective of the work reported here was to develop a closed loop analytic model, incorporating a model for the human pilot (namely, the optimal control model), that would allow certain simulation design tradeoffs to be evaluated quantitatively and to apply this model to analyze a realistic flight control problem. The effort concentrated on the dynamic, closed loop aspects of

*The work described herein was performed under Contract No. NSA1-14449 for NASA - Langley Research Center. Mr. Russell Parrish was the Technical Monitor and contributed many helpful suggestions.

the simulation. Problems associated with perceptual issues in cue generation were not considered. However, the limitations imposed by the dynamics of visual cue generation equipment are considered and the model can be readily extended to incorporate the dynamics associated with motion simulation.

The optimal control model of the human operator[3,4] is central to the closed loop analysis techniques that have been employed. This model has been validated and applied extensively and has a structure that is well-suited to analysis of the simulation problems of interest. The model can be used to generate predictions of attentional workload as well as of closed-loop performance. This is significant because, as noted earlier, pilots may compensate for simulation shortcomings but with a workload penalty; such simulation-induced operator tradeoffs need to be explored.

Two approaches to closed-loop modelling are considered. The first employs a continuous approximation to the open-loop dynamics of the digital simulation in conjunction with the standard OCM. The second model attempts to represent the discrete simulation dynamics more exactly. It utilizes a simulation version of the OCM. This latter model is referred to as the hybrid model.

In the remainder of this paper, the closed loop models are described and some results of applying the models are presented and discussed. More extensive discussion and additional results may be found in Reference 5.

2. CONTINUOUS CLOSED LOOP MODEL

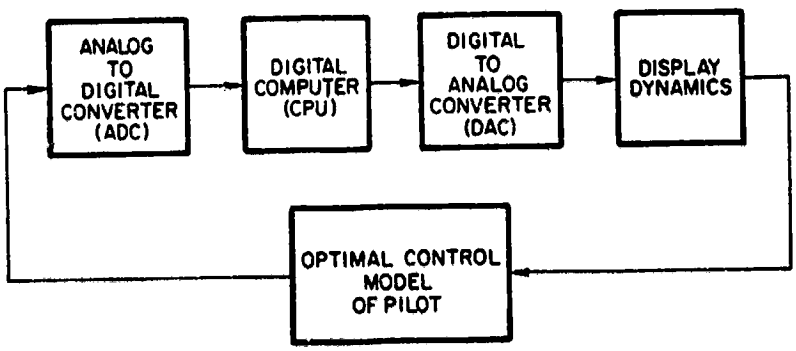

Figure 1. Simplified Model for Closed Loop Analysis of Digital Simulation

Figure 1 is a block diagram of a simplified closed-loop model for analyzing problems in digital, piloted simulation. The pilot model in Figure 1 is the OCM.[3,4] The elements corresponding to the simulator are an analog-to-digital converter (ADC), a digital computer (CPU), a digital-to-analog converter (DAC) and a visual display system. Briefly, the ADC is a sampler preceded by a

low-pass filter included to minimize aliasing effects, the CPU implements difference equations so as to simulate the vehicle's response to the pilot's (sampled) input, the DAC is a data-hold (either zero-order or first-order), and the visual display system is a servo-driven projector that continuously displays target position (relative to the aircraft) to the pilot. These elements will be discussed in more detail below.

2.1 Optimal Control Model for Pilot

Some of the features of the OCM that are particularly relevant to subsequent discussions are reviewed briefly here. Figure 2 illustrates the

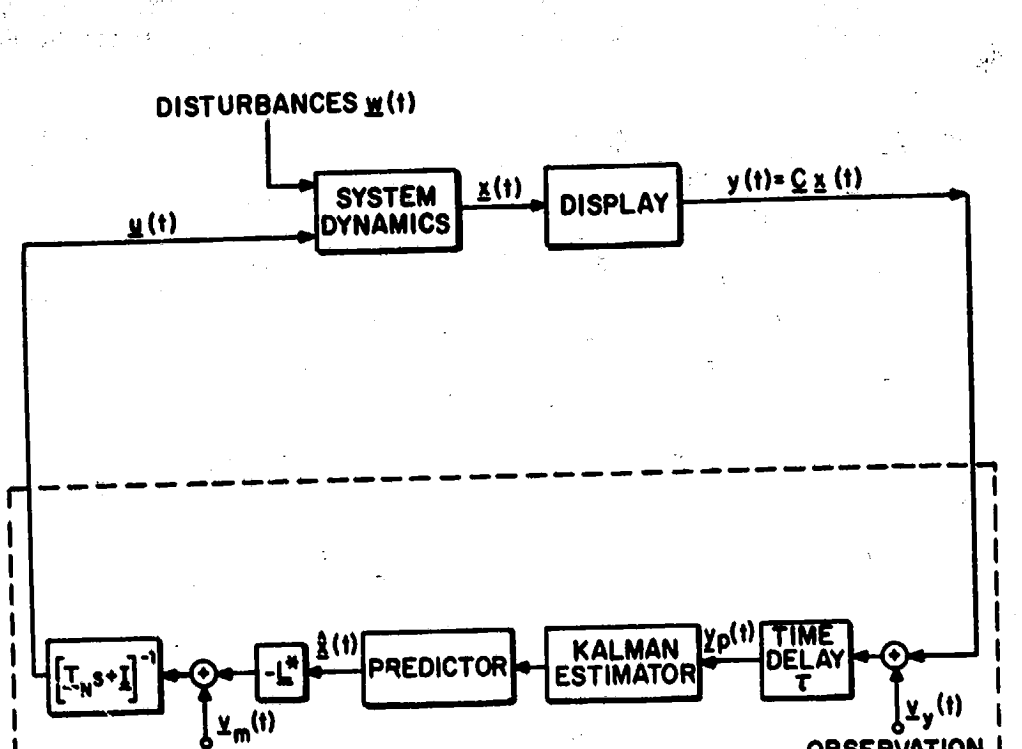

Figure 2. Structure of Optimal Control Model

structure of the OCM.

The OCM as originally conceived and developed presupposes that the system dynamics, corresponding to the element to be controlled, may be expressed in state variable format

$$\dot{\mathbf{x}}(t) = \mathbf{A}_c\mathbf{x}(t) + \mathbf{B}_c\mathbf{u}(t) + \mathbf{E}_c\,\mathbf{w}(t)$$
$$\mathbf{y}(t) = \mathbf{C}_c\mathbf{x}(t) + \mathbf{D}_c\mathbf{u}(t) \qquad (1)$$

where $\mathbf{x}$ is the n-dimensional state-vector, $\mathbf{y}$ is an m-dimensional vector of displayed outputs, $\mathbf{u}$ is the r-dimensional control input vector and $\mathbf{w}$ is a vector of disturbance and/or command inputs. The system matrices ($\mathbf{A}_c$, $\mathbf{B}_c$, $\mathbf{C}_c$, $\mathbf{D}_c$, $\mathbf{E}_c$) are generally assumed to be time-invariant, although this restriction can be relaxed. The above system dynamics include the linearized dynamics of the aircraft (or other controlled element) and any dynamics associated with measurement, control and display systems. The subscript c on the system matrices is included to emphasize that the dynamics are assumed to represent a continuous system.

For purposes of discussion it is convenient to consider the model for the pilot as being comprised of the following: (i) an "equivalent" perceptual model that translates displayed variables into noisy, **delayed** perceived variables denoted by $\mathbf{y}_p$ (t); (ii) an information processing model that attempts to estimate the system state from the perceived data. The information processor consists of an optimal (Kalman) estimator and predictor and it generates the minimum-variance estimate $\hat{\mathbf{x}}(t)$ of x(t); (iii) a set of "optimal gains", $\mathbf{L}^*$, chosen to minimize a quadratic cost functional that expresses task requirements; and (iv) an equivalent "motor" or output model that accounts for "bandwidth" limitations (frequently associated with neuromotor dynamics) of the human and an inability to generate noise-free control inputs.

The time delay or transport lag is intended to model delays associated with the human. All displayed variables are assumed to be delayed by the same amount, viz. τ seconds. However, delays introduced by the simulation can be added to the human's delay without any problem, so long as all outputs are delayed by the same amount. If such is not the case, then all outputs can be delayed by τ , where τ is now the sum of the minimal delay introduced by the simulation and the operator's delay, and additional delays for the outputs requiring them can be modeled via inclusion of Pade approximations in the output path.

The observation and motor noises model human controller remnant and involve injection of wide-band noise into the system. This noise is "filtered" by the other processes in the pilot model and by the system dynamics. It should be emphasized that the injected remnant is a legitimate (if unwanted) part of the pilot's input to the system and, therefore, significant amounts of remnant power should not be filtered out in the de-aliasing process of a valid simulation.

The neuro-motor lag matrix limits the bandwidth of the model response. Typically, for wide-band control tasks, involving a single control variable, a bandwidth limitation of about 10-12 rad/sec gives a good match to experimental results (i.e., a neuro-motor time constant of $T_N \simeq .08 - .10$). For many

aircraft control tasks there is no significant gain (i.e., reduction in error) to be obtained by operating at this bandwidth, and there can be some penalty in unnecessary control activity. For such tasks larger time constants (lower bandwidths) have been observed. In these cases, if the neuro-motor time constant is arbitrarily set at the human's limit (say $T_N \simeq .1$) good predictions of tracking or regulation performance are usually obtained; but the control activity and pilot bandwidth tend to be overestimated. Inasmuch as it may be useful to have more accurate estimates of pilot bandwidth for making decisions concerning approximations to the discrete simulations, T_N was chosen in this study on the basis of a model analysis of the tradeoff between error and control-rate scores. Essentially, this involves using the model to sweep out a curve of error-score versus control-rate score to find the value of T_n where marginal improvements in performance require substantial increases in rms control-rate (the "knee" of the curve). A value of approximately .15 sec (an operator bandwidth of about 1 Hz) was determined on the basis of this analysis.[5]

The optimal estimator, predictor and gain matrix represent the set of "adjustments" or "adaptations" by which the human attempts to optimize performance. The general expressions for these model elements depend on the system and task and are determined by solving an appropriate optimization problem according to well-defined rules. Of special interest here is that, in the basic continuous OCM, the estimator and predictor contain "internal models" of the system to be controlled and the control gains are computed based on knowledge of system dynamics. The assumption is that the operator learns these dynamics during training.*

The question arises as to the appropriate internal model when the human controls a discrete simulation of a nominally continuous system. It would appear that if the operator is trained on the simulation, then the appropriate model corresponds to the simulation model.** This will be the assumption employed with the continuous model.

Finally, it should be mentioned that the solution to the aforementioned optimization problem yields predictions of the complete closed-loop performance statistics of the system. Predictions of pilot describing functions and control and error spectra are also available. All statistical computations are performed using covariance propagation methods, thus avoiding costly Monte Carlo simulations. This is not the case for the hybrid model described later.

*This is generally more convenient than assuming that the external model differs from the true model and also leads to good performance prediction.[6]

**If the simulation model is poor, a control strategy that is inappropriate for the actual system could be learned with negative results in, say, transfer of training. This issue can be addressed with the hybrid model described later.

2.2 Open-Loop Simulator Dynamics

The application of the standard OCM to closed-loop analysis requires a continuous state representation of the complete controlled element. Since the human pilot in closed loop control will operate on essentially continuous outputs to generate continuous control inputs even when digital computers are used in the aircraft simulation, it is meaningful to consider a continuous transfer function approximation to the open loop simulation dynamics. Such an approximation is developed here. It consists of a rational transfer function multiplied by a transportation lag. The rational transfer function approximates the amplitude distortions introduced by discrete integration of the flight dynamics. The delay accounts for all the phase lags introduced by the simulator components. These phase lags are the major source of degraded performance and increased workload in closed loop tasks. However, the amplitude distortions can be significant for open-loop responses.

System Function From Stick Input to Displayed Output

Figure 3 is an elaborated diagram of the simulator portion of Figure 1.

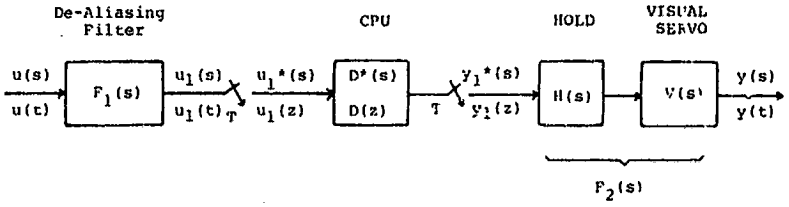

Figure 3. Open Loop Simulator Dynamics

Note that the output of the visual servo, y(t), is a continuous signal as is the input, u(t), to the A-D dealiasing pre-filter.* For analysis purposes we use the notation implied in Figure 3. Variables or functions with argument s represent Laplace transforms and those with argument z correspond to z-transforms. The starred quantities correspond to Laplace transforms of impulse sampled signals or of functions of z and are defined, e.g., by[7]

$$u_1^*(s) \triangleq u_1(z)\Big|_{z=e^{sT}} = \frac{1}{T}\sum_{n=-\infty}^{\infty} u_1(s+jn\Omega) \qquad (2)$$

or

*For simplicity, we consider single-input, single-output systems. The results obtained here can be generalized to more complex situations.

$$D^*(s) = D(z)\Big|_{z=e^{sT}} \tag{3}$$

where T is the sample period and

$$\Omega = \frac{2\pi}{T} = \text{sampling frequency} \tag{4}$$

From Figure 3, we obtain

$$y(s) = F_2(s)y_1^*(s) = F_2(s)D^*(s)u_1^*(s)$$

$$= F_2(s)D^*(s)\ \frac{1}{T}\sum_{n=-\infty}^{\infty} F_1(s+jn\Omega)\,u(s+jn\Omega) \tag{5}$$

Equation (5) gives the exact transfer relation between u(s) and y(s). However, it is not a useful expression from the standpoint of closed-loop modeling because of the infinite summation.

The system function for a linear system (such as the simulation system under analysis) may be obtained by computing the steady-state response of the system to an input of the form exp(st). It is shown in Reference 5 that the system function from u(s) to y(s) (in steady-state) is periodic in time with a period equal to the sampling period. However, if the output y(t) is considered only at sampling instants, which amounts to introducing a "fictitious" sampler at the output[7] then the following time-independent transfer function is obtained.

$$G(s;t)\Big|_{\substack{\text{sample}\\ \text{times}}} = G(s) = F_2^*(s)D^*(s)F_1(s) \tag{6}$$

We shall consider G(s) defined in (6) to be the "exact" transfer function for the simulation. Note that $F_2^*(s) = (VH_1)^*(s)$.

Equation (6) is intractable for use with the continuous OCM. Therefore, it will be necessary to approximate (6) for closed-loop analysis. A straightforward approximation is to ignore all but the n=0 term in the expression for F_2^* which results in

$$G(s) \approx \frac{F_2(s)D^*(s)F_1(s)}{T} = \frac{V(s)H_i(s)D^*(s)F_1(s)}{T} \qquad (7)$$

In utilizing (7) it will be necessary to approximate D*(s); the procedure for doing this will be discussed subsequently.

For the simulator of interest here,[8] the transfer functions for the de-aliasing filter and servo are, respectively,

$$F_1(s) = \frac{\omega_c^3}{s^3 + 2\omega_c s^2 + 2\omega_c^2 s + \omega_c^3} \qquad (8)$$

$$V(s) = \frac{\omega_n^2}{s^2 + 2\zeta\omega_n s + \omega_n^2} \qquad (9)$$

The hold transfer function is either

$$H_o(s) = \frac{1-e^{-sT}}{s} \qquad (10)$$

or

$$H(s) = T(1+Ts)\left(\frac{1-e^{-Ts}}{Ts}\right)^2 \qquad (11)$$

Sample periods, T, of 1/32, 1/16, 1/10 will be considered as these cover the likely range of interest for piloted simulation. Therefore, if the cutoff of the de-aliasing filter is chosen on the basis of the sampling theorem, $\omega_c >$ 5Hz. The visual servo dynamics of interest are characterized by $\omega_n = 25$ rad/sec and $\zeta = .707$.[8]

With these parameter values, each of the transfer functions of (8) - (11) may be approximated reasonably well by a pure transport lag in the frequency region of interest for manual control ($\omega <$ 10 rad/sec). That is,

$$F_1(s) \approx e^{-\tau_F s}$$
$$V(s) \approx e^{-\tau_V s} \qquad (12)$$
$$H_o(s) \approx e^{-\tau_o s}$$
$$H_1(s) \approx e^{-\tau_1 s}$$

where

$$\tau_F \approx \frac{2}{\omega_c} = \frac{2T}{\pi} \qquad \tau_o = T/2$$
$$\tau_V \approx (\zeta\omega_n)^{-1} = .057 \text{ sec} \qquad \tau_1 = T \qquad (13)$$

Substitution of (12) into (7) yields

$$F_1(s)D^*(s)F_2(s) \approx D^*(s) \exp\left[-(\tau_F + \tau_V + \tau_i)s\right] \qquad (14)$$

where i = 0 or 1 for the zero-order or first-order hold, respectively.

2.3 Effects of Discrete Integration

In the previous section the transfer function $D^*(s)$ was left unspecified as was the manner in which it was to be approximated for continuous closed-loop analysis with the OCM. In general, $D^*(s)$ will be a "distorted" version of the continuous system dynamics that are to be simulated. Some general features of the distortions introduced by various integration schemes are analyzed and presented in Reference 5 along with results pertinent to the F-8 dynamics that are to be analyzed later. Here, we present a brief discussion of the general effects of discrete integration followed by a description of the method that will be used to approximate $D^*(s)$ in the continuous closed-loop analysis.

Consider the continuous vehicle-dynamics as described in the state-variable form of Equation (1). For constant system matrices, the transfer matrix between system outputs and control inputs is given by

$$\mathbf{y}(s) = \mathbf{G}_c(s)\,\mathbf{u}(s)$$
$$\mathbf{G}_c(s) = \mathbf{C}_c(s\mathbf{I}-\mathbf{A}_c)^{-1}\mathbf{B}_c + \mathbf{D}_c \qquad (15)$$

When equations (1) are "integrated" digitally, they lead to a discrete approximation with the following transfer matrix[5]

$$D^*(s) = \left\{\mathbf{c}_d[z\mathbf{I}-\mathbf{A}_d]^{-1}\,\mathbf{B}_d + \mathbf{D}_d\right\}\Big|_{z=e^{sT}} \qquad (16)$$

where the matrices in (16) depend on the particular integration scheme and sample period as well as on the corresponding continuous system matrices. Several points concerning Equation (16) are noteworthy. First, the elements of the discrete transfer matrix $D^*(s)$, cannot, in general, be expressed as the ratio of two polynomials in s of finite degree. Second, the Bode responses corresponding to (16) will differ from the continuous responses in both amplitude and phase; and, further, the responses for the discrete system are periodic in frequency with period equal to $2\pi/T$. Third, the poles and zeros of Equation (16) are infinite in number and are given by, for example,

$$P_i = \sigma_i + j(\omega_i + 2\pi k);\ k = 0, \pm 1, \pm 2, \ldots$$

Moreover, the principal values for the poles and zeros, i.e., those with $k = 0$, are not, in general, equal to the corresponding poles and zeros of the continuous system. Finally, simple integration schemes, such as Euler, will have the same number of principal poles as the continuous system, whereas multi-step integration schemes, like (Adams-Bashforth), will introduce principal roots that are spurious.

We now turn to the problem of approximating $D^*(s)$ so that the continuous representation of the simulator dynamics may be completed. Because of the restrictions imposed by the OCM, we restrict the possible approximations to the following form:

$$\frac{Y_i}{u_j} = D^*_{ij}(s) \approx \tilde{D}_{ij}(s)e^{-\tau_c s}$$

where $\tilde{D}(s)$ is a ratio of finite polynomials in s with numerator degree less than or equal to the degree of the denominator. Note that the same "computation" delay, τ_c is associated with each transfer function. This turns out to be a good approximation for the dynamics considered in Section 4. If different delays were needed, they would be included in $\tilde{D}$ via a rational Pade approximation.[5]

The simplest approach to selecting $\tilde{D}$ is to use (15) and let

$$\tilde{D}_{ij}(s) = \Phi_{C_{ij}}(s) \tag{17}$$

From the standpoint of the OCM, this means that the state equations for the original dynamics are used and discrete integration is modeled by adding a delay determined from the phase distortion. As has been stated earlier, such an approximation probably accounts for the major source of difficulty of discrete integration in closed-loop control. However, to employ it exclusively is to leave us somewhat uncertain as to the closed-loop significance of the amplitude distortions.

It was found[5] that very good approximations to discrete Bode responses could be obtained for the longitudinal control tasks that are to be analyzed later. These approximations involved perturbation of aircraft stability derivatives and CAS parameters to yield continuous modes that agreed with the discrete modes. In the case of A-B integration, it was also necessary to introduce a zero in the continuous vehicle transfer in order to reproduce the amplitude distortion introduced by this integration scheme.

When Equation (17) is substituted in (14), the basic result is that for the frequency range likely to be of interest in continuous aircraft control problems, the simulator transfer function can be modelled as

$$\frac{Y(s)}{u(s)} = \tilde{D}(s)e^{-\tau_s s} \tag{18}$$

where D(s) is an "approximation" to the Bode response for digital integration of the vehicle dynamics. The simulator delay, is given by

$$\tau_s = \tau_F + \tau_H + \tau_V + \tau_C \tag{19}$$

where τ_F, τ_H, τ_V and τ_C respectively, are the delays introduced by the de-aliasing filter, hold, visual servo and CPU (discrete integration).

The approximation of Equation (18) readily lends itself to efficient application of the OCM. The system matrices corresponding to a state representation of $\tilde{D}$ and the values for τ_s are easily obtained for different sample periods, etc. For each condition, a single run of the OCM is sufficient to predict the corresponding performance. Adjustment of pilot parameters, specifically observation noise levels, allows the sensitivity to pilot attention to be examined.[9]

3. THE HYBRID MODEL

There are shortcomings in the continuous model. For example, the effects of aliasing are not considered. Thus, the degrading effects of the de-aliasing filter are included in the continuous model but not its benefits. This means that decreasing the bandwidth, ω_c, of that filter can only lead to negative results, a situation that is not obviously true, in general. Similarly, because only the delays inherent in the data holds are considered, zero-order holds will always show less degradation than first-order holds. But, in some instances, the first order hold may provide advantages that outweigh the additional delay penalty. This type of trade-off cannot be explored with the continuous OCM without more sophisticated approximation to the simulator dynamics. Because of these and other potential shortcomings, it was decided to develop a hybrid model.

The approach to developing the hybrid model is to "simulate" the closed-loop simulation. A discrete simulation version of the OCM[10] was used in a closed-loop digital Monte Carlo type computation* in which "continuous" elements of the loop are updated at a rate significantly greater than discrete elements. In other words, the hybrid model is a multi-rate sampling system, rather than a true hybrid system. (Informal experimentation indicates that a sample rate five times that of the discrete elements is adequate to simulate continuity for the cases considered here.) In addition, to different sample rates for continuous and discrete elements, the updating of the discrete equations of the hybrid model is different for the two kinds of elements. In particular, discrete elements are updated by means of the integration scheme and time-step specified for the "true" simulation. The equations for continuous elements are updated at the faster rate via transition matrix methods.

The equations describing the hybrid model are quite complex and are described in detail in Reference 5. Here, we simply note two features of the model that are interesting and useful in subsequent analyses. First, the hybrid model was implemented so that the prediction time in the predictor of the OCM (See Figure 2) could be selected arbitrarily. This contrasts with the standard OCM in which the prediction time is always equal to the time delay. This additional freedom allows us to "sweep out" curves of performance versus prediction time. Theoretically, best performance should be obtained when the prediction time is equal to the sum of the human's delay and the simulator's delay, i.e. when the operator compensates optimally for both delays. Since the human's delay is an assumed parameter, the compensation time for best performance yields an independent measure of the simulator delay.

A second feature of the hybrid model is that the internal model for the OCM need not be the same as the system model.* This flexibility provides the hybrid model with a capability for examining transfer-of-training questions. In addition, since optimal performance should correspond to the operator's model being equivalent to the system model, the hybrid model can be used to evaluate different (internal) approximations to the discrete simulation.

A final point concerning the hybrid model is worth noting. Because it is a Monte Carlo model, it normally will require many computer solutions to obtain meaningful statistics. In the analyses to be performed here, however, we are interested in the steady-state response of stationary systems. Rather than average over many Monte Carlo solutions, we have assumed ergodicity of the processes and utilized time-averaging of a single response. Even with this simplification, it is fairly expensive computationally to obtain valid statistical results.[5]

*A truly hybrid (analog/digital) model is possible but would require a hybrid computer (which was not available).
*Indeed, the system model can even be nonlinear.

4. AN EXAMPLE

The models for closed-loop analysis of simulator effects have been applied to an "example" simulation involving air-to-air target tracking. Results have been obtained for both longitudinal and lateral control tasks, for augmented and unaugmented dynamics and for different target motions. In addition, the effects of changes in design parameters of each simulation component have been explored. The full range of results may be found in Reference 5. Here, a sample of the results is presented to show the extent of the simulation effects and the capabilities of the closed-loop models.

4.1 The Tracking Problem

Figure 4 shows the geometry of the air-to-air tracking in the longitudinal plane. The gunsight is assumed to be fixed and aligned with the aircraft body axis. For longitudinal tracking, we will assume that no information concerning the target's pitch angle, ϕ nor the relative aspect angle is available. The pilot's task is assumed to be that of minimizing the mean-squared, line-of-sight

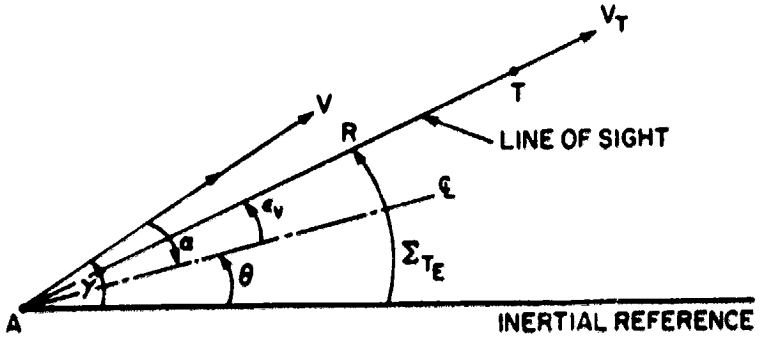

Σ_{T_E} = INERTIAL LINE-OF-SIGHT ANGLE (ELEVATION)
R = TARGET RANGE
ϵ_v = ELEVATION TRACKING ERROR = $\Sigma_{T_E} - \theta$

Figure 4. Target Geometry

tracking error ϵ_v.

The target is assumed to execute random vertical evasive maneuvers. In particular, target altitude variations are generated by passing white, gaussian noise through a third order filter as illustrated below.

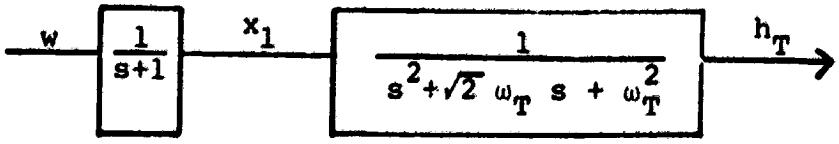

By selecting the covariance of the white noise and the cutoff frequency of the Butterworth filter, rms altitude variations and normal accelerations may be specified. Here, a cutoff frequency of $_t$ = .5 rad/sec was used and the noise covariance was chosen to give an rms altitude variation of 267 ft. and an rms acceleration of 3.1 g. Of course, the linearity of the problem allows us to scale the results to correspond to higher or lower accelerations.

The longitudinal short-period dynamics of the F8 without augmentation will be the baseline dynamics. The relevant equations may be found in Reference 5. The short period dynamics have a natural frequency of 2.28 rad/sec and a damping coefficient of .29; this represents poor short period handling qualities.[2] Because of this, and because we are interested in the effects of simulation parameters as a function aircraft dynamics, a set of augmented longitudinal dynamics will also be considered. A pitch command augmentation system (CAS) is used to modify the base airframe characteristics. The CAS design is a modified version of the design proposed in Reference 11.

The equations for the augmented dynamics are given in Reference 5. The F8 with the pitch CAS has short period roots with a natural frequency of 2.78 rad/sec and a damping coefficient of .64; this constitutes a significant improvement in the short period handling qualities.[2]

5. MODEL RESULTS

5.1 Continuous Model

The continuous model was used to analyze the effects of both simulation parameters and problem variables. With respect to the simulation, the effects of sample period and integration scheme are presented for the longitudinal CAS-OFF dynamics. Problem dependent effects are illustrated by comparing CAS-OFF and CAS-ON results.

We define a basic simulation configuration, corresponding to Figure 3, in which the cutoff of the de-aliasing filter is set at half the sample frequency, the visual servo has the DMS characteristics (ζ = .707, ω_n = 25 rad/sec), and a zero-order hold is used in data reconstruction.

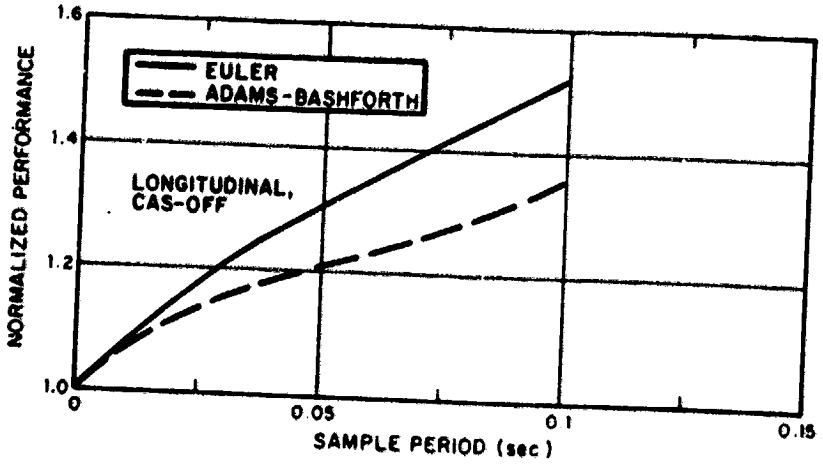

Figure 5. Effect of Discrete Simulation on Normalized Performance

Figure 5 gives normalized performance for the basic configuration as a function of sample period and integration scheme. Normalized performance is defined as the tracking error obtained for the simulation configuration divided by the tracking error that would be obtained in a continuous simulation with no delays (or in flight).* The normalization is determined by computing the performance utilizing the original, continuous state equations and assuming the only delay is that of the operator (.2 seconds).

Figure 5 shows substantial effects are introduced by the simulation, particularly at low sample rates. Even for the highest sample rate (T = .03125), there is a 16-20 percent performance degradation. A change of this magnitude exceeds the normal intra- and inter-subject variability in manual tracking tasks and would, therefore, be expected to be significant. For the lowest sample rates the performance degradation ranges from 35-50 percent, numbers that are clearly consequential. It is clear that, from a closed-loop tracking standpoint, A-B integration is superior to Euler integration.

The results in Figure 5 assume that the only adjustments in pilot strategy resulting from the simulation are an increase in prediction time to compensate for simulator delays and the adoption of an internal model that accounts for the amplitude distortions (and pole perturbations) introduced by the CPU. The results are based on the assumption of a fixed level of attention throughout. However, the pilot may choose to devote more attention to the task (work harder) and, thereby, reduce tracking error. A reasonable question to ask, then, is "How much more attention to the task would be required to achieve performance levels comparable to those that could be obtained in a continuous simulation?" This question can be addressed using the model for workload associated with the OCM.[9] The result of this analysis is shown in Figure 6.

*As might be the case in an all analog simulation with analog displays providing undelayed visual information.

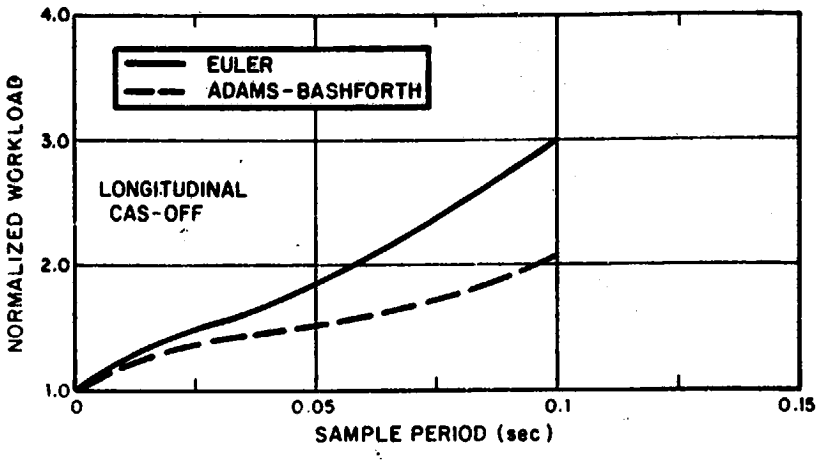

Figure 6. Simulation Workload Penalty

It can be seen from Figure 6 that to achieve the performance equivalent to that for continuous simulation, the pilot would have to increase his attentional workload by factors up to three for the conditions considered. There is a substantial workload penalty and it might be expected that a compromise between performance degradation and increased workload might evolve. This would be the case, especially if the pilot had not flown the vehicle or a continuous simulator in the same task so that there would be no basis for setting a criterion level of performance.

Before leaving the workload question, a further point is worth noting. In the describing function literature, it has been common practice to associate workload with the generation of lead. However, there has been no quantitative connection between the amount of lead and the increase in workload. In the present context, one can think of the increased prediction time necessary to compensate for simulator delays as imposing a (processing) workload analogous to that of lead generation. The measure of attentional workload given previously may then be thought of as an alternative means of quantifying the workload imposed by the requirement for additional prediction.

It was anticipated that there would be an interaction between the effects of simulation parameters and problem variables such as vehicle handling qualities. Thus, the above tracking task was analyzed for the CAS/ON configuration.

Figure 7 compares normalized longitudinal CAS-ON and CAS-OFF performance for the basic simulation. It can be seen that the CAS-ON performance is degraded more by the discrete simulation than the CAS-OFF performance. These results are explained by the fact that the delays introduced by digital integration are larger for CAS-ON dynamics than they are for CAS-OFF dynamics. The effects of longitudinal dynamics when viewed in terms of absolute performance are interesting and are also shown in Figure 7. The absolute performance for continuous simulation is better for CAS-ON than CAS-OFF (by about 3.5 percent) and the sensitivity to incremental computation delay is about

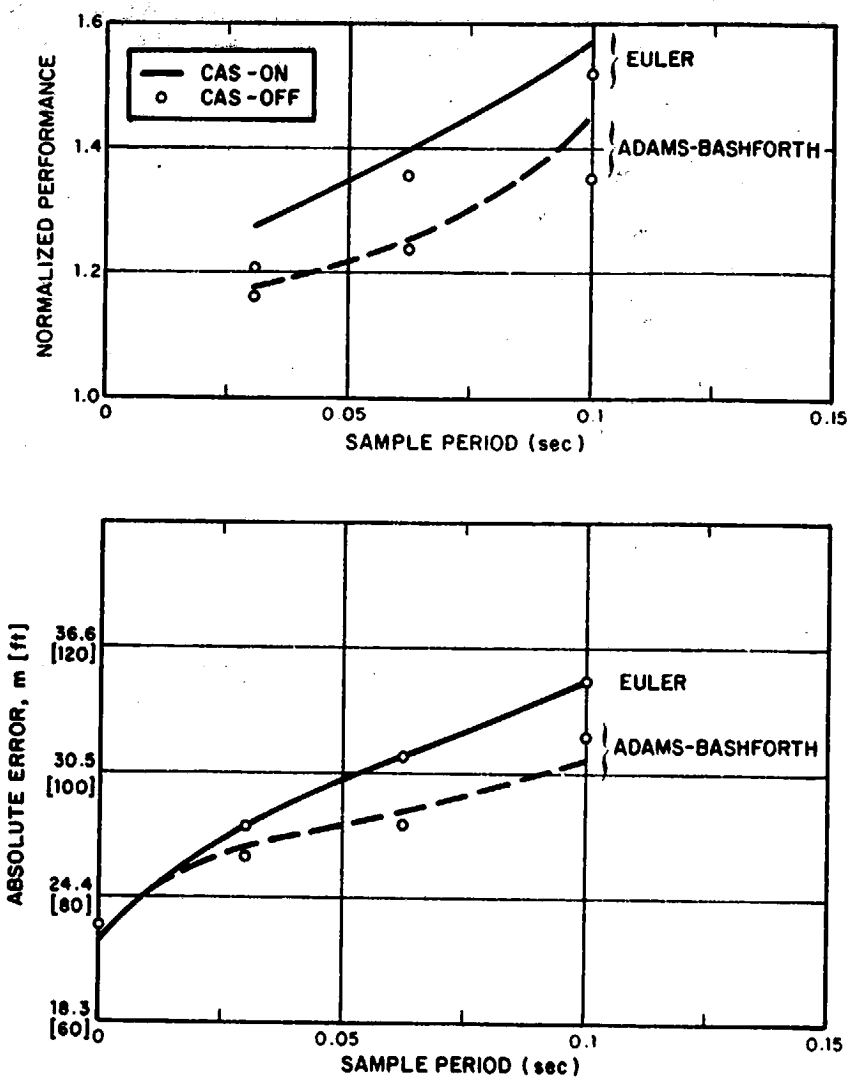

Figure 7. Effect of Vehicle Dynamics

the same for the two configurations. Thus, for a given simulation configuration, absolute performance for CAS-ON and CAS-OFF configurations will be about the same if Euler integration is used and the CAS-OFF configuration can give better performance if A-B integration is used. In other words, the discrete simulation washes out any improvement due to the CAS!

5.2 Hybrid Model

The hybrid model was used to investigate several issues that could not be examined readily in the continuous model context. Results were limited to the longitudinal unaugmented dynamics because of cost and time considerations

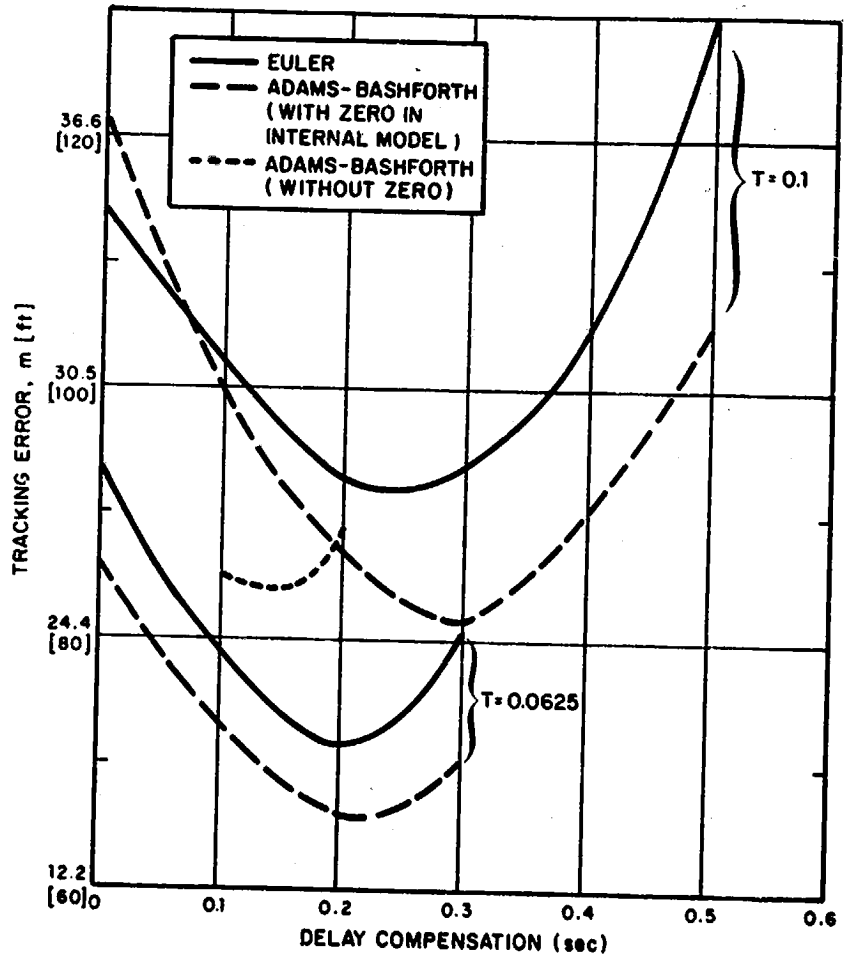

Figure 8. Effect of Operator Prediction Time

Figure 8 shows the sensitivity of performance to delay compensation time* for the basic simulation configurations with both Euler and A-B integration and

*The prediction time in excess of that needed to compensate for the operator's intrinsic delay of .2 sec.

for T = .1 and T = .0625. The "internal" models for the OCM in these cases are the continuous approximations to the discrete transfers that incorporate amplitude distortion effects; however, no delay is added to the human's delay of .2 seconds to account for the simulations delays. Thus, we expect the optimal prediction times to be approximately equal to the delay introduced by the simulation. This is indeed the case as can be seen in Figure 8. For Euler integration the minima occur at ~.26 sec and ~.2 sec. for T = .1 and .0625, respectively; the corresponding simulation delays are .27 and .19 .

For A-B integration the minima are at larger compensation times than for Euler. This is a result of the method used to account for amplitude distortion. (Recall that a zero was introduced in the transfer function and this necessitated an increased transport delay to match the phase lag at mid-frequencies.) With T = .1, the optimal prediction time is around .3 seconds and the simulation delay is ~.32 seconds. For T = .0625, performance does not appear to be very sensitive to prediction time in the neighborhood of the optimum. The simulation delay is ~.21 seconds and performance for this prediction time is indistinguishable from optimal performance. Figure 8 also shows a curve for the case where the operator's internal model does not include a zero to match the amplitude distortion of A-B integration. It can be seen that for this case a delay compensation of only ~.17 seconds is required. This corresponds to the delays introduced by the servo, pre-filter and zero-order hold. The optimal performance is marginally poorer than for the case with amplitude distortion included in the internal model. These results suggest that although including the zero provides a better model of the effect of A-B integration, the increased delay compensation needed to offset the extra lead should not be viewed here as a workload penalty.

These results confirm the estimates of simulation delay used in the continuous model. They also demonstrate implicitly how operators may adapt their behavior to compensate for simulator inadequacy. The added prediction required may impose a workload penalty as noted earlier.

Another form of adaptation to the simulation involves the pilots internal model. Two questions are of interest: 1.) What model will the trained operator adopt when "flying" the simulator?; and 2.) What is the "transfer" effect of a wrong model when transitioning from discrete simulator to continuous simulator (flight)? At least partial answers to these questions for the longitudinal dynamics and Euler integration are provided by the results shown in Figure 9.

Figure 9 gives performance vs. delay compensation for T = .1 and two internal models. One internal model is that derived to match the corresponding discrete transfer function while the other is the basic continuous model. It can be seen that better performance is obtained when the internal model corresponds to the approximate discrete model implying that this is a better model of the discrete simulation than is the original continuous model. Figure 9 also shows the effect of using the model corresponding to T = .1 seconds in a simulation where the actual sample period is .03125 seconds (i.e., nearly continuous) as compared to using the model for T = .03125 seconds (i.e., the correct one). If the operator optimizes delay compensation, performance will be degraded by about 10%. If, on the other hand, the delay compensation appropriate to T = .1 is used, a performance penalty of about 19% will be incurred. The effect is not substantial here but it might be in other tasks.

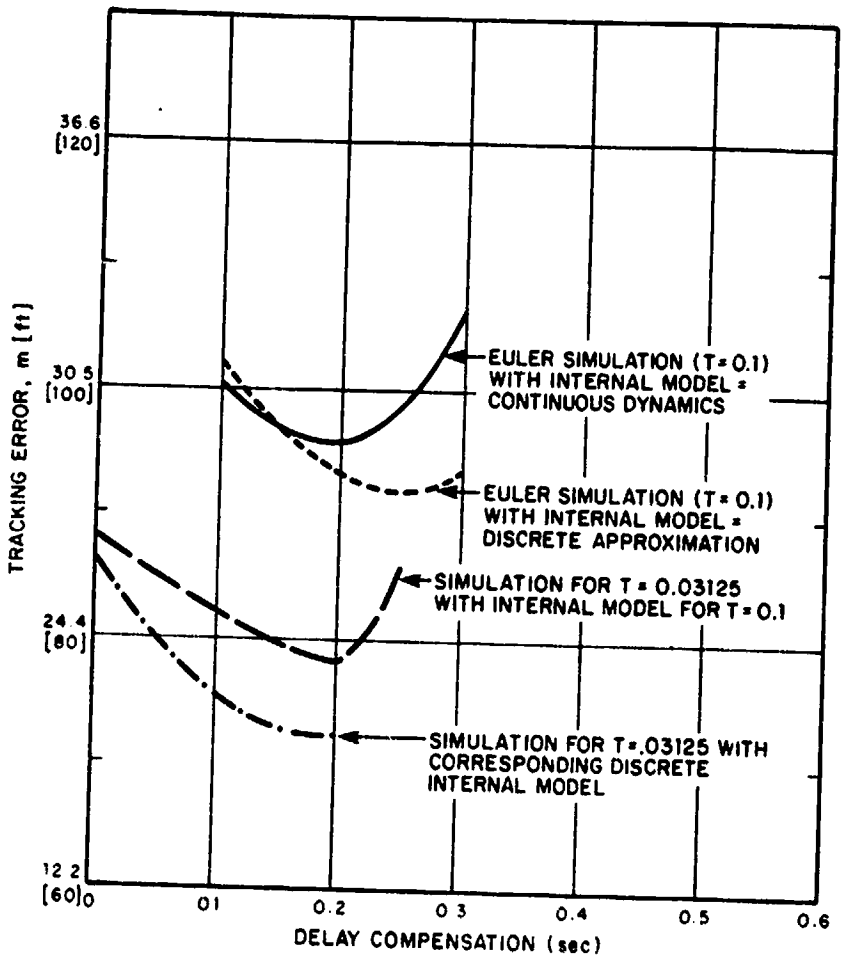

Figure 9. Effect of Internal Model

The effect of the cutoff frequency of the de-aliasing filter on performance is shown in Figure 10. Euler integration of the vehicle equations is used and other simulation parameters correspond to the basic configuration. The results are for a sample frequency of 10 Hz (T = .1) so a cutoff frequency of ω_c = 5 Hz satisfies the Nyquist requirement. Results are obtained for ω_c = 1, 5 and 20 Hz, respectively. The lowest value of ω_c = 20 Hz is based on the assumption that there is not significant signal power beyond 5 Hz so there is no need to set the filter break-point at that frequency and incur the delay penalty. The results in Figure 10 favor using the higher cutoff frequency, ω_c = 20 Hz, for this problem. Furthermore, there is a substantial penalty for using the low frequency cutoff. These two results imply that aliasing is not a problem here. We also note that the performance minima for ω_c = 20 Hz and 5 Hz occur at about the correct value of prediction time; the optimum prediction time for $_c$ = 1 Hz

is much larger but not quite so large as the estimated total simulation delay of

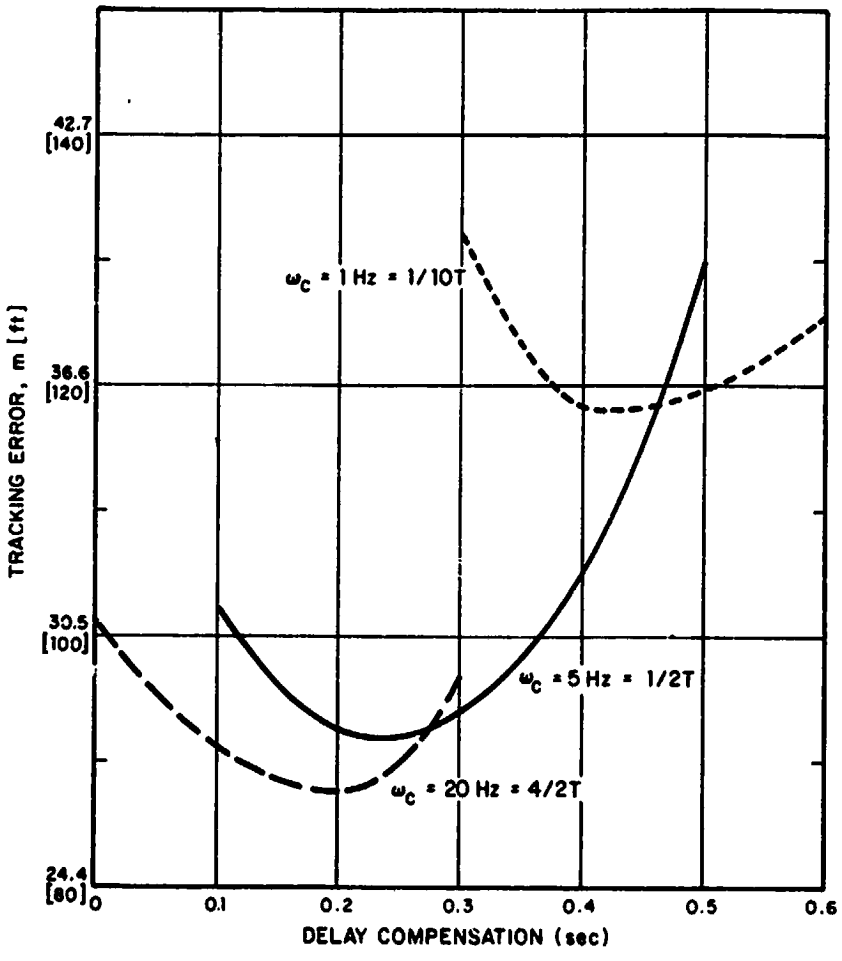

Figure 10. Effect of Dealiasing Filter Cutoff Frequency

.53 seconds.

The effects of using a first order hold instead of a zero order hold are shown in Figure 11 for both Euler and A-B integration at T = .1 and for Euler integration at T = .0625. The corresponding best zero order hold performance values are also shown for comparison purposes. At a sample period of .1 seconds, slightly lower tracking errors are obtained for Euler integration with a first order hold than with a zero order hold; in addition, the minimum performance is obtained with less delay compensation. The situation for A-B integration and a .1 second sample period is the reverse of that for Euler. That is, for A-B integration the first order hold degrades performance.

A possible explanation for these results is as follows. The first order hold uses intersample information which provides some lead. For long sample

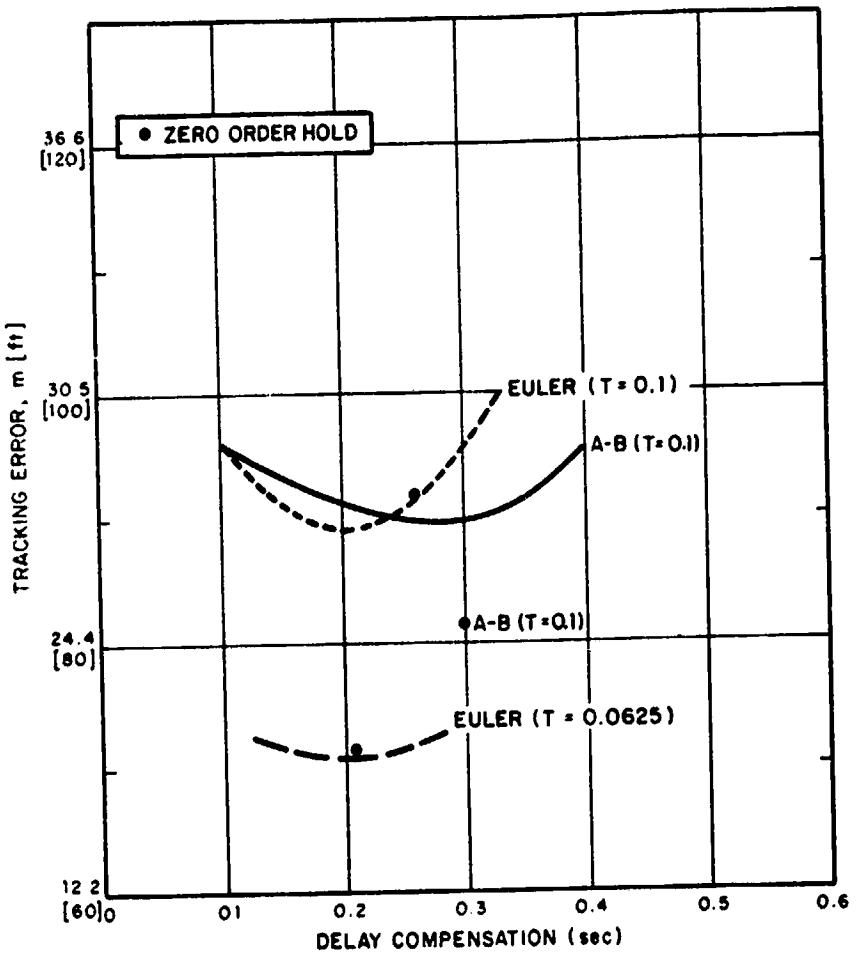

Figure 11. Effect of First Order Hold

periods and Euler integration, the effective lead provided is apparently more beneficial than the lag penalty associated with the higher order hold. The beneficial effects of a first order hold should decrease as the sample period decreases. This is supported by the results for T = .0625 which show no difference between the two holds. In the case of A-B integration the added delay of the first order hold dominates. This may be due to A-B integration having an implicit first order hold at the input, thereby reducing any advantage in adding such a hold at the output.

6. SUMMARY AND CONCLUSIONS

In this paper we have examined the effects of simulation parameters and components on simulator fidelity, particularly with regard to predicting operator performance and workload. Our focus has been on the dynamical aspects of simulator primarily as they relate to closed loop control. We have generally ignored questions that would necessitate inclusion of detailed models for cue perception leaving these to future study.

An approximate continuous model of the discrete simulation was incorporated in the standard optimal control model for the human operator. The resulting continuous closed-loop model was used to analyze both overall simulation effects and the effects of individual elements. The results showed that, as compared to an ideal continuous simulation, the discrete simulation could result in significant performance and/or workload penalties. The magnitude of the effects depended strongly on sample period as expected. From a closed-loop standpoint it seemed clear that A-B integration was much to be preferred. With respect to the other simulation components it can be said that any reduction in delay is desirable. Such reductions inevitably involve increased costs (hardware or software) which must be balanced against the expected improvements.

In addition to the continuous model, a hybrid model was developed to allow investigation of situations that could not be treated adequately with the continuous model. Several interesting results were obtained with this model. It was shown that for this (fairly typical) aircraft control problem signal bandwidths were such that the de-aliasing filter cutoff frequency could be set at a value greater than half the sample frequency. Also, there appeared to be a potential under certain conditions for improved simulator performance with a first order hold (rather than a zero order hold). The model was also used to show demonstrable effects for adopting the simulator dynamics as an internal model. The need to compensate for simulator delays via added prediction was also shown.

We believe the models developed here can be very useful in developing engineering requirements for flight simulators. These requirements will be problem dependent which is one reason why models are needed. As we see it now, the process for using the models would involve the following steps:

i) Use standard OCM to analyze ideal continuous simulation to develop baseline performance and to determine expected signal bandwidths.

ii) Analyze distortion introduced by discrete integration schemes and develop continuous models for discrete dynamics valid over the band of interest.

iii) Analyze effects of integration, cue dynamics etc. using continuous model.

iv) Use hybrid model to examine effects of data reconstruction, de-aliasing cutoff frequency etc.

Before this procedure could be used with complete confidence the models described herein need further validation and extension. It is especially important to collect data in a carefully controlled experiment to verify the individual simulation effects.

REFERENCES

1. Gum, D. R. and W. B. Albury, "Time-Delay Problems Encountered in Integrating the Advanced Simulator for Undergraduate Pilot Training," **Journal of Aircraft**, Vol. 14, No. 4, April 1977.

2. Queijo, M. J. and D. R. Riley, "Fixed-Base Simulator Study of the Effect of Time Delays in Visual Cues on Pilot Tracking Performance," NASA TN D-8001, October 1975.

3. Kleinman, D. L., S. Baron and W. H. Levison, "An Optimal Control Model of Human Response," **Automatica**, Vol. 6, No. 3, pp. 367-384, May 1970.

4. Baron, S., "A Model for Human control and Monitoring Based on Modern Control Theory", **Journal of Cybernetics and Information Science**, Vol. 1, No. 1, Spring 1976.

5. Baron, S., R. Muralidharan and D. L. Kleinman, "Closed Loop Models for Analyzing Engineering Requirements for Simulators", Bolt Beranek and Newman Inc., Report No. 3718, May 1978.

6. Baron, S. and J. Berliner, "The Effects of Deviate Internal Representations in the Optimal Model of the Human Operator," **Proceedings of Thirteenth Annual Conference on Manual Control**, M.I.T., Cambridge, Mass., June 1977.

7. Rosko, J.S., "Digital Simulation of Physical Systems" Addison-Wesley Publishing Co., Reading, Mass., 1972.

8. Ashworth, B.R. and W. M. Kahlbaum, Jr., "Description and Performance of the Langley Differential Maneuvering Simulator," NASA TN D-7304, NASA, Langley Research Center, June 1973.

9. Levison, W. H., J. I. Elkind and J. L. Ward, "Studies of Multi-Variable Manual Control Systems: A Model for Task Interference," NASA CR-1746, May 1971.

10. Kleinman, D. L., S. Baron and J. Berliner, "MCARLO: A Computer Program for Generating Monte-Carlo Trajectories in a Time-Varying Man-Machine Control Task," U.S. Army Missile Research and Development Command, Tech. Report TD-CR-77-2, Redstone Arsenal, Ala., June 1977.

11. Hartmann, G. L., J. A. Hauge and R. C. Hendrick, "F-8C Digital CCV Flight Control Laws," NASA CR-2629, February 1976.